24th INTERNATIONAL CONGRESS ON SOUND AND VIBRATION
23–27 July 2017, London

ICSV24
23-27JULY 2017
LONDON CALLING

SOUND ABSORPTION OF MICRO-PERFORATED PANEL PRODUCED BY ADDITIVE MANUFACTURING

Zhengqing Liu, Mohammad Fard, Xiaojing Liu

RMIT University, School of Engineering (SENG), Melbourne, VIC 3083, Australia
email: liu.zhengqing@rmit.edu.au

John Laurence Davy

RMIT University, School of Science, Melbourne, VIC 3001, Australia

Jiaxing Zhan

DSI Holdings Pty Limited, Melbourne, VIC 3171, Australia

This paper investigates the sound absorption of a multilayer acoustic absorber. The acoustic absorber is consisting of a 3D printed micro-perforated panel, a porous sound absorbing material and an air cavity mounted in front of a rigid wall. The micro-perforated panel specimens are printed with various thickness, hole spacing, and diameters. The sound absorption coefficients of the acoustic absorbers are experimentally measured by using a two-microphone impedance tube method. The experimentally obtained sound absorption coefficients are theoretically validated by using the transfer matrix method. The comparisons show that the measured sound absorption coefficients agree fairly well with the prediction results. By adjusting the hole spacing, hole diameter, and thickness of the micro-perforated panel, an acoustic absorber with high sound absorption peaks can be implemented. The significant improvement of the sound absorption of the acoustic absorber at low to mid frequencies can be attributed to the porous sound absorbing material and the air cavity. The results in this paper provide a new approach to produce micro-perforated sound absorbers for acoustic applications.

Keywords: micro-perforated panel; porous material; impedance tube method; sound absorption

1. Introduction

The micro-perforated sound absorber is usually a thin panel with a large number of submillimetre perforations in the front of a rigidly backed air cavity. According to Maa's [1] research with regard to the acoustic properties of the micro-perforated panels that by providing the correct acoustical resistance and lower the acoustic reactance, the wide-band sound absorptions can be further enhanced. Nowadays, it has been widely applied within acoustic designs to tune the sound absorption peak frequency and to protect the interior trim materials (e.g. porous sound absorbing material). In general, obtaining desired sound absorption by altering geometric design is relatively easy, however it is rather difficult and costly to process such small size of holes by adopting traditional manufacturing methods, e.g. etching, micro-punch and laser technology. Furthermore, the conventional methods may lead to veneer tear out, partially plugged, tapered, and rough walls, which may have a significant effect on the acoustic performance of a sound absorber.

Some of the literature has presented feasible methods to produce a micro-perforated panel, such as using the infiltration method [2], the MEMS technology [3], and the use of parallel perforated ceramic materials [4]. On the other hand, the actual drilling shapes were usually used instead of conventional circular holes, e.g. slits were punched to reduce the manufacturing process and cost [5,

6]. The acoustic behavior of a micro-slit sound absorber was presented by Maa [7], and the acoustic properties of a micro-perforated panel with arbitrary cross-sectional perforations were derived by Ning et al. [8]. Furthermore, the composite acoustic absorption structure was optimized for specific noise control applications. Wang et al. [9] developed a new multilayer acoustic absorption structure via a bionic method, where the sound attenuation for broadband and low-frequency noises was significantly improved. Kim et al. [10] developed a composite helical shaped porous sound absorbing structure by using carbon fiber to enhance the sound absorption. It was lighter and thinner in comparison with conventional materials. Li et al. [11] have been able to improve the low-frequency sound absorption by using a perforated panel with extended tubes (PPET). And most recently, an alternative method of using 3D printing technology to fabricate a high precision sound absorber was introduced and first studied by Liu et al. [12, 13].

In this paper, the micro-perforated panels were produced using 3D printing technology. The structure of a single micro-perforated layer backed with a porous sound absorbing material and an air cavity were studied. This type of structure is frequently used in building designs and vehicle interior trim designs. Their sound absorption coefficients were both experimentally measured and theoretically predicted. The acoustic properties of the theoretical model and its measured results are presented and discussed in order to quantify effects of the design parameters within the micro-perforated panels.

2. Measurement

2.1 3D printed specimen

Figure 1 shows a few of the 3D printed micro-perforated panel specimens and the porous sound absorbing material used in this study. It uses stereolithography (SLA) technology to produce higher precision level of micro-perforated panel test specimens through the layer by layer approach by using ultraviolet light. In this study, the test specimens were printed with a fine layer resolution of 25.4 µm.

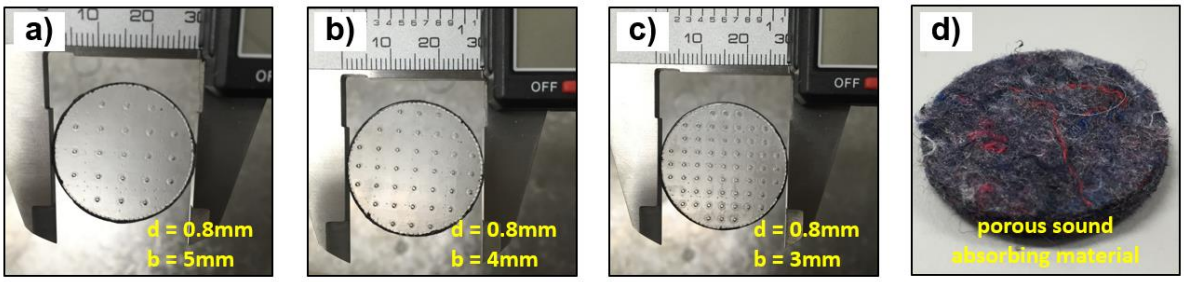

Figure 1: 3D printed micro-perforated panel samples, (a) S#1; (b) S#2; (c) S#3 and (d) porous material.

Thickness and diameters of the specimens and the hole diameters within the samples are 1 mm, 29 mm, and 0.6 mm and 0.8 mm, respectively. The test specimens were printed with different hole spacings (b = 5 mm, 4 mm, 3 mm) to provide a range of open area ratios. The structural parameters of the 3D printed micro-perforated panel specimens are listed in Table 1.

Table 1: Measured structural parameters for the 3D printed micro-perforated test specimens.

specimens	hole diameter, d (mm)	hole spacing, b (mm)	open area ratio, p (%)
S#1	0.8	5	1.6
S#2	0.8	4	2.8
S#3	0.8	3	4.6
S#4	0.6	5	0.9
S#5	0.6	4	1.6
S#6	0.6	3	2.6

Moreover, a 4.5 mm non-woven porous sound absorbing material is punched to produce a 29 mm diameter test specimen which can be fitted within the impedance tube. This porous sound absorbing material has an average density of 96.6 kg/m^3. The acoustic properties of the selected porous sound absorbing material were: airflow resistivity σ = 289,000 N·s/m^4, tortuosity α_∞ = 1.46, porosity ϕ = 0.85, the viscous and thermal characteristic lengths are Λ = 112 μm and Λ' = 224 μm, respectively. These acoustic material properties were already measured, studied and reported by Liu et al. [14, 15].

2.2 Sound absorption coefficient measurement

The sound absorption coefficient was experimentally measured according to the ASTM E1050-12 standard [16] by using the two-microphone impedance tube method. Figure 2 shows the schematic diagram of the two-microphone impedance tube method, where a B&K impedance tube Type 4206 was used to while measuring the sound absorption coefficient of the test specimens. The inner diameter of the B&K impedance tube was 29 mm, and the sound absorption coefficients were measured across the frequency range from 500 Hz to 6400 Hz.

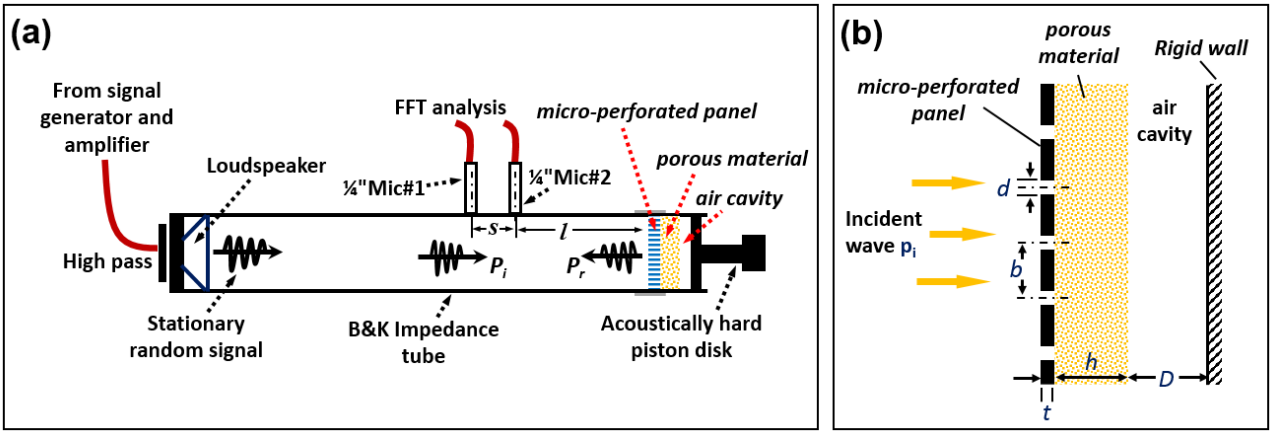

Figure 2: (a) schematic diagram of the two-microphone impedance tube method and (b) schematic of a micro-perforated panel combined with a porous sound absorbing material and an air cavity.

In this method, a random sound signal was generated by a loudspeaker, the incident (P_i) and reflected (P_r) components were determined from the relationship between the acoustic pressure measured by the two microphones. The complex sound reflection coefficient R of a test specimen was calculated from the corrected complex acoustic transfer function H_{12} between the two microphone. The normal sound absorption coefficient α_n was calculated by $\alpha_n = 1-|R|^2$. In this study, the acoustic absorber used is consisting of a micro-perforated layer, a porous sound absorbing layer and a 5mm air cavity behind the porous sound absorbing material.

3. Theoretical model

The transfer matrix method (TMM) is applied and used to predict the theoretical sound absorption coefficient of a sound absorber which includes a micro-perforated layer, a porous sound absorbing material, and an air cavity. In this study, the global transfer matrix T_{Total} of a sound absorber can be obtained by connecting the individual transfer matrices T_M (micro-perforated panel), T_P (porous sound absorbing material layer) and T_A (air cavity) in order, and the corresponding matrices are [17-21]:

$$T_{\mathrm{M}} = \begin{bmatrix} 1 & Z_M \\ 0 & 1 \end{bmatrix}. \tag{1}$$

$$T_{\mathrm{P}} = \begin{bmatrix} \cos(k_c h) & jZ_P \sin(k_c h) \\ j\sin(k_c h)/Z_P & \cos(k_c h) \end{bmatrix}. \tag{2}$$

$$T_{\mathrm{A}} = \begin{bmatrix} \cos(k_0 D) & jZ_0 \sin(k_0 D) \\ j\sin(k_0 D)/Z_0 & \cos(k_0 D) \end{bmatrix}. \tag{3}$$

$$T_{\mathrm{Total}} = T_{\mathrm{M}} \cdot T_{\mathrm{P}} \cdot T_{\mathrm{A}} = \begin{bmatrix} T_{11} & T_{12} \\ T_{21} & T_{22} \end{bmatrix}. \tag{4}$$

where Z_M is the acoustic impedance of a micro-perforated panel [17], Z_P is the acoustic impedance of the porous sound absorbing material [18-21], and Z_0 is the acoustic impedance of air, which is given by $Z_0 = \rho_0 c_0$ (ρ_0 is the air density, c_0 is the velocity of sound in air). k_0 is the wave number of the air cavity in front of the rigid wall, and it is given by $k_0 = 2\pi f$. k_c is the complex wave number of the sound waves in the porous sound absorbing material. h is the thickness of the porous sound absorbing material, and D is the thickness of the air cavity. The surface impedance Z_s and the sound absorption coefficient of a multilayer sound absorber then can be calculated by:

$$Z_{\mathrm{s}} = T_{11}/T_{21}. \tag{5}$$

$$\alpha_n = \frac{4\,\mathrm{Re}(Z_{\mathrm{s}}/\rho_0 c_0)}{\left[1+\mathrm{Re}(Z_{\mathrm{s}}/\rho_0 c_0)\right]^2 + \left[\mathrm{Im}(Z_{\mathrm{s}}/\rho_0 c_0)\right]^2}. \tag{6}$$

4. Results and discussion

4.1 Comparison of the results

Figure 3 and Figure 4 compare the predicted and measured sound absorption coefficient graphs (one-third octave band) for 0.8 mm hole diameter micro-perforated panel, and 0.6 mm hole diameter micro-perforated panel backed by a porous sound absorbing material and 5 mm air cavity, respectively.

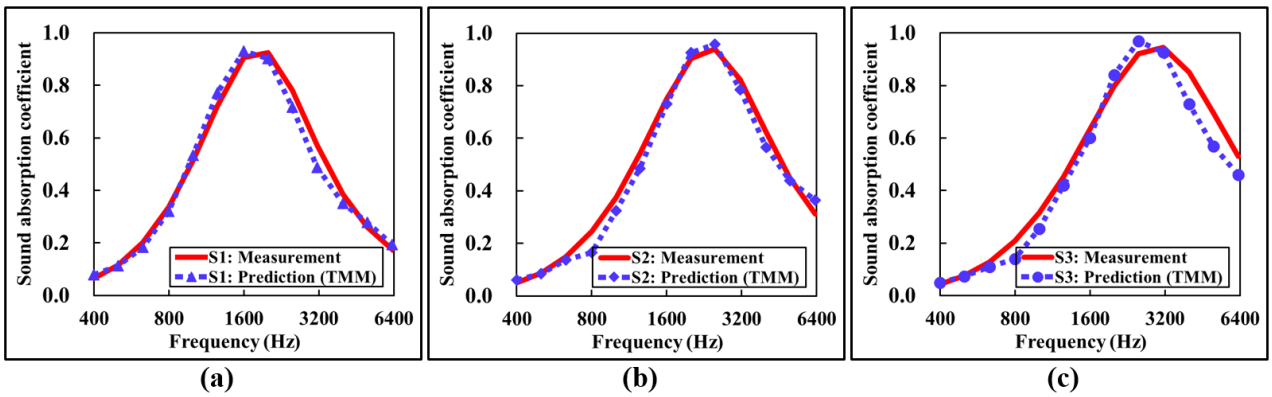

Figure 3: Comparison of the sound absorption coefficient from the measurement and prediction of a micro-perforated panel (d = 0.8 mm) backed by a porous sound absorbing material and 5 mm air cavity, (a) S#1, b = 5 mm; (b) S#2, b = 4 mm and (c) S#3, b = 3 mm.

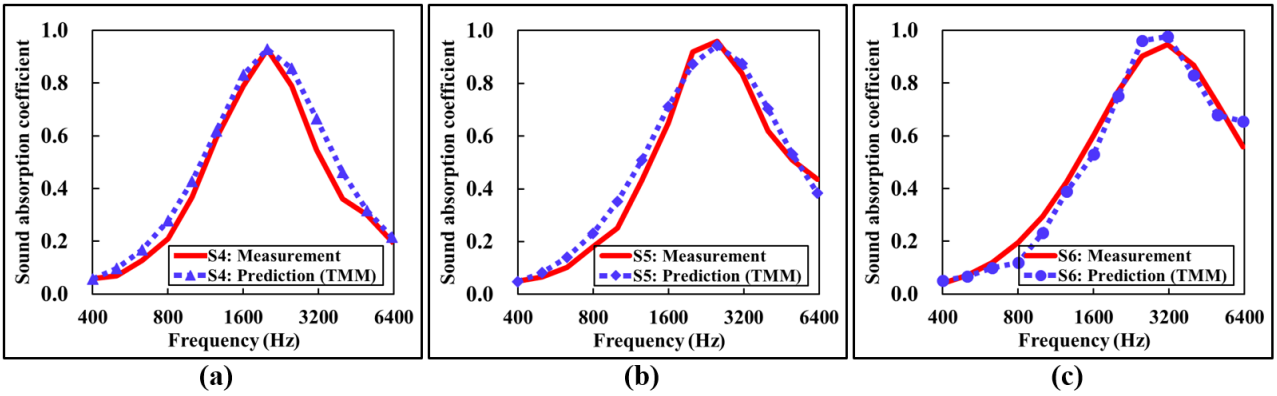

Figure 4: Comparison of the sound absorption coefficient from the measurement and prediction of a micro-perforated panel (d = 0.6 mm) backed by a porous sound absorbing material and 5 mm air cavity, (a) S#4, b = 5 mm; (b) S#5, b = 4 mm; and (c) S#6, b = 3 mm.

The results shown that the sound absorption coefficient graphs (one-third octave band) obtained by the prediction method agree reasonably well with the measured results. The predicted peak sound absorption coefficient values, as well as their corresponding frequencies also agree fairly well with the measured data. This confirms that the micro-perforated panel layer can be precisely fabricated using additive manufacture method and it could also provide predictable acoustic absorption performance when backed by a porous sound absorbing material and air cavity.

4.2 Effect of open area ratio

Figure 5 shows the variation of the sound absorption coefficient of the micro-perforated panel (d = 0.8 mm and d = 0.6 mm) as the open area ratio of the micro-perforated layer increases. The results show that increasing the open area ratio of the micro-perforated layer yields a higher acoustic resonance frequency for the peak sound absorption coefficient. This has been proved to be true for both cases where d = 0.8 mm and d = 0.6 mm micro-perforated panels were backed by a porous sound absorbing material and an air cavity of 5 mm. This is due to an increase in the open area ratio results in the decrease of the total acoustic mass of all the holes, and thus increases the resonant frequency at which the peak the sound absorption coefficient occurs. Furthermore, the porous sound absorbing material and air cavity behind the micro-perforated panel can produce wider sound absorption bandwidth at high frequencies.

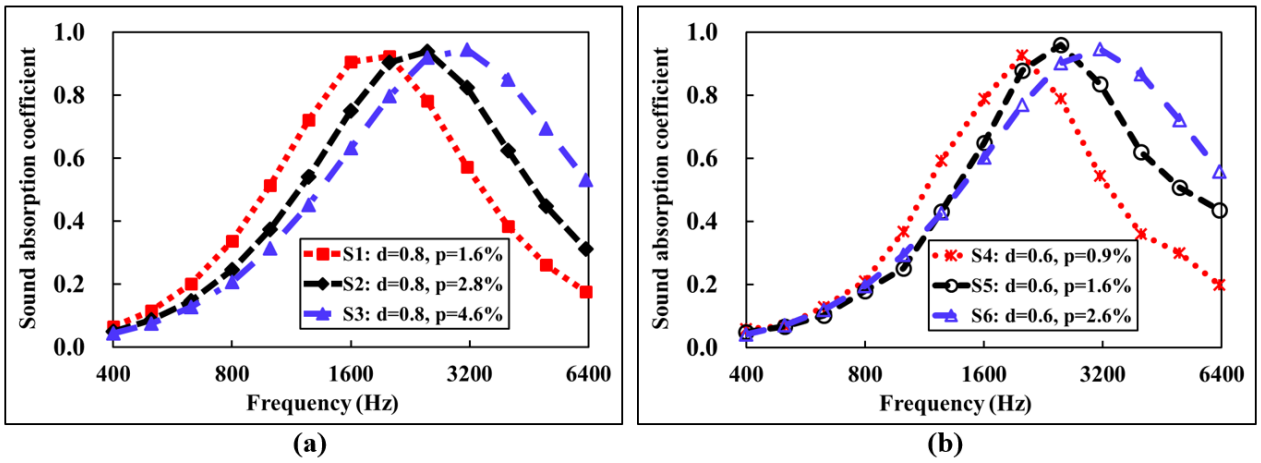

Figure 5: Influence of open area ratio on the sound absorption coefficient for (a) d = 0.8 mm micro-perforated panel and (b) d = 0.6 mm micro-perforated panel, backed by a porous sound absorbing material and 5 mm air cavity.

4.3 Effect of hole diameter and thickness

The effect of the hole diameter and the panel thickness on the sound absorption coefficient of the 3D printed micro-perforated layer when backed by a porous sound absorbing material and 5 mm air cavity, is shown in Figure 6. In Figure 6 (a), all the sample have the identical thickness of t = 1 mm and hole spacing of b = 4 mm. Within the Figure 6 (b), all the sample have the constant hole diameter of d = 0.6 mm and hole spacing of b = 4 mm. It can be observed that the acoustic resonance frequency for the peak sound absorption coefficients shifts towards the high-frequency range, along with the increase of the hole diameter and thickness of the micro-perforated panel. However, it appears that using the same hole spacing and panel thickness but different hole diameter provides very similar sound absorption curve. In addition, reducing the thickness of the micro-perforated panel has significantly improve the peak sound absorption coefficient value at high-frequency range.

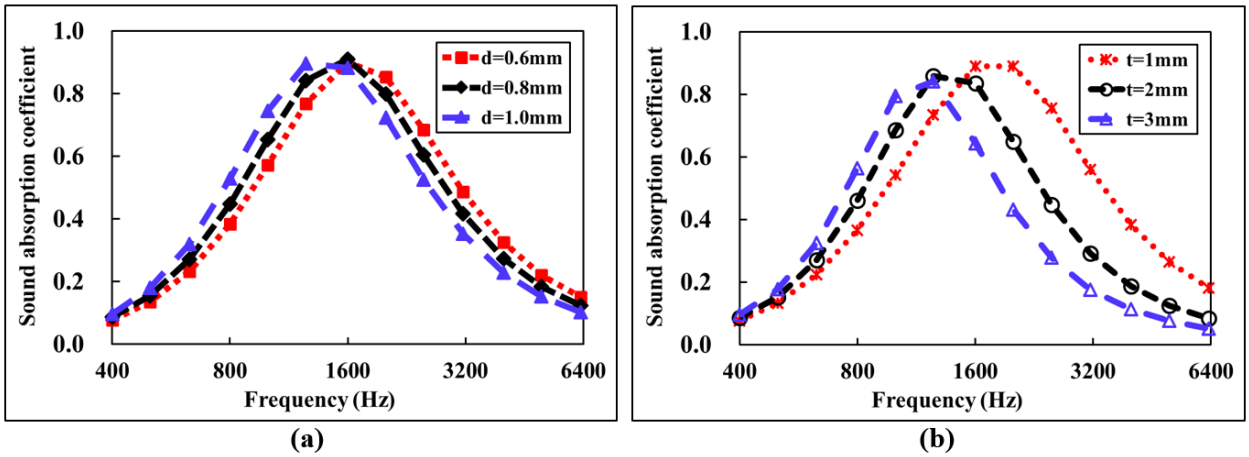

Figure 6: Influence of (a) hole diameter and (b) thickness on the sound absorption coefficient for the 3D printed micro-perforated panel when backed by a porous sound absorbing material and 5 mm air cavity.

5. Conclusions

This paper investigated the sound absorption coefficient of a 3D printed micro-perforated panel which is backed by a porous sound absorbing material and an air cavity. It is shown that a micro-perforated layer can be produced using additive manufacture method. The sound absorption coefficient of a 3D printed micro-perforated layer backed with a porous sound absorbing material and air cavity is measured and theoretically predicted. It has been shown that the measured results agree fairly well with the theoretically predicted model. The influences of the main design parameters, e.g. panel thickness, hole spacing and diameter are presented. In order to obtain the desired peak acoustic absorption frequency as well as a wider frequency range, it is effective and achievable by either adjusting the hole spacing of the micro-perforated layer or form a combination structure by adopting appropriate porous sound absorbing material layer and an air cavity. To enhance the sound absorption coefficient and peak acoustic absorption frequency further, suitable value of hole diameter and panel thickness should be chosen.

ACKNOWLEDGMENTS

The authors would like to thank *Excellerate Australia Ltd* and *Futuris Automotive Group* for their financial support for this research. Zhengqing Liu is grateful to technical staffs at *RMIT University*, Mr. Patrick Wilkins, Mr. Peter Tkatchyk and Mr. Julian Bradler in preparing a series of specimens and experiments.

REFERENCES

1 Maa, D. Y. Potential of microperforated panel absorber, *The Journal of the Acoustical Society of America*, **104** (5), 2861–2866, (1998).

2 Cobo, P. and Espinosa, F. M. Proposal of cheap microperforated panel absorbers manufactured by infiltration, *Applied Acoustics*, **74** (9), 1069–1075, (2013).

3 Qian, Y. J., Kong, D. Y., Liu, S. M., Sun, S. M. and Zhao, Z. Investigation on micro-perforated panel absorber with ultra-micro perforations, *Applied Acoustics*, **74** (7), 931–935, (2013).

4 Yang, D., Wang, X. and Zhu, M. The impact of the neck material on the sound absorption performance of Helmholtz resonators, *Journal of Sound and Vibration*, **333** (25), 6843–6857, (2014).

5 Kristiansen, U. R. and Vigran, T. E. On the design of resonant absorbers using a slotted plate, *Applied Acoustics*, **43** (1), 39–48, (1994).

6 Stinson, M. R. The propagation of plane sound waves in narrow and wide circular tubes, and generalization to uniform tubes of arbitrary cross-sectional shape, *The Journal of the Acoustical Society of America*, **89** (2), 550–558, (1991).

7 Maa, D. Y. Theory of microslit absorbers, *Acta Acustica*, **25** (6), 481–485, (2000).

8 Ning, J. F., Ren, S. W. and Zhao, G. P. Acoustic properties of micro-perforated panel absorber having arbitrary cross-sectional perforations, *Applied Acoustics*, **111**, 135–142, (2016).

9 Wang, Y., Zhang, C., Ren, L., Ichchou, M., Galland, M. A. and Bareille, O. Sound absorption of a new bionic multi-layer absorber, *Composite Structure*, **108**, 400–408, (2014).

10 Kim, B. S., Cho, S. J., Min, D. K. and Park, J. Sound absorption structure in helical shapes made using fibrous paper, *Composite Structure*, **134**, 90–94, (2015).

11 Li, D., Chang, D. and Liu, B. Enhancing the low frequency sound absorption of a perforated panel by parallel-arranged extended tubes, *Applied Acoustics*, **102**, 126–132, (2016).

12 Liu, Z., Zhan, J., Fard, M. and Davy, J. L. Acoustic properties of a porous polycarbonate material produced by additive manufacturing, *Materials Letters*, **181**, 296–299, (2016).

13 Liu, Z., Zhan, J., Fard, M. and Davy, J. L. Acoustic properties of multilayer sound absorbers with a 3D printed micro-perforated panel, *Applied Acoustics*, **121**, 25–32, (2017).

14 Liu, Z., Fard, M. and Davy, J. L. The effects of porous materials on the noise inside a box cavity, *Proceedings of the 22nd International Congress on Sound and Vibration*, Florence, Italy, 12–16 July, (2015).

15 Liu, Z., Fard, M. and Davy, J. L. Acoustic properties of the porous material in a car cabin model, *Proceedings of the 23rd International Congress on Sound and Vibration*, Athens, Greece, 10–14 July, (2016).

16 ASTM E1050-12. Standard test method for impedance and absorption of acoustical materials using a tube, two microphones and a digital frequency analysis system. New York: American National Standards Institution; 2012.

17 Song, B. H. and Bolton, J. S. A transfer-matrix approach for estimating the characteristic impedance and wave numbers of limp and rigid porous materials, *The Journal of the Acoustical Society of America*, **107** (3), 1131–1152, (2000).

18 Ruiz, H., Cobo, P., Dupont, T., Martin, B. and Leclaire, P. Acoustic properties of plates with unevenly distributed macroperforations backed by woven meshes, *The Journal of the Acoustical Society of America*, **132** (5), 3138–3147, (2012).

19 Johnson, D. L., Koplik, J. and Dashen. R. Theory of dynamic permeability and tortuosity in fluid-saturated porous-media, *Journal of Fluid Mechanics*, **176**, 379–402, (1987).

20 Champoux, Y. and Allard, J. F. Dynamic tortuosity and bulk modulus in air-saturated porous-media, *Journal of Applied Physics*, **70** (4), 1975–1979, (1991).

21 Allard, J. F. and Champoux. Y. New empirical equations for sound propagation in rigid frame fibrous materials, *The Journal of the Acoustical Society of America*, **91** (6), 3346–3353, (1992).